WITHDRAWN: Mg-doped NiO Nanoparticles Decorated Multi-Walled Carbon Nanotube (MWCNT) Nanocomposite and their Biological Activities

Noor Q. Ali
Applied Sciences Department, University of Technology, Baghdad 100001, Iraq
Ali A. Taha
Applied Sciences Department, University of Technology, Baghdad 100001, Iraq
Mustafa K. A. Mohammed
mustafa_kareem97@yahoo.com
Applied Sciences Department, University of Technology, Baghdad 100001, Iraq https://orcid.org/0000-0002-1850-6355
Ihab Q. Ali
Al-Esraa University Collage, Medical Lab. Technique, Baghdad, Iraq
Duha S. Ahmed
Computer Sciences Department, Dijlah University College, Al-Masafi Street, Al-Dora, Baghdad 00964, Iraq

Research Article

Keywords: MCF-7 cell, Carbon nanotubes, Sol-Gel method, Nickle oxide, Anticancer activity

Posted Date: June 22nd, 2021

DOI: https://doi.org/10.21203/rs.3.rs-632388/v1

EDITORIAL NOTE:

The full text of this preprint has been withdrawn by the authors while they make corrections to the work. Therefore, the authors do not wish this work to be cited as a reference. Questions should be directed to the corresponding author.

Abstract

Here we report a novel nanocomposite composed from Mg-doped NiO and Mg-doped\MWCNT using a facile sol-gel method. The synthesized Mg-doped NiO and Mg-doped\MWCNT nanocomposite was characterization by XRD diffraction (XRD), energy dispersive spectroscopy (EDS), Fourier transform infrared spectroscopy (FTIR), scanning electron microscopy (SEM), and UV–Vis spectrophotometer. The X-Ray analysis revealed that the formation of nanocomposites, which has a cubic phase and a high crystalline nature. The FE-SEM images confirmed the success of decoration the 6%Mg- doped NiO on the surface of the treated MWCNT through the emergence of spherical shapes over the cylindrical tubes. Conversely, optical measurements reveal that the energy gap value for the Mg-NiO and the Mg/NiO-MWCNT nanocomposite are 3.28 and 2.82 eV, respectively. This indicates decreasing the zone between conduction band and valance band. Moreover, it found that Mg doped NiO\MWCNT nanocomposite showed high removal efficiency towards the lead element compared with the Mg-doped NiO. Also, MTT test was employed to study antitumor activity against MCF-7 and WRL68 cells. Our results showed that the Mg doped NiO-MWCNT had cell viability of 66.7 and 71.9% against MCF-7 and WRL68, respectively. Whereas, Mg-doped NiO sample showed cell viability of 70.2 and 71.9% against MCF-7 and WRL68, respectively.

Highlights

- The Mg-doped NiO NPs and Mg-doped NiO\MWCNTs nanocomposites were synthesized by using sol-gel rout.
- The anticancer activity of prepared nanocomposites was studied against MCF-7 and WRL68 cells.
- The effectiveness of nanostructures towards removing lead (Pb^{+2}) from contaminated water was studied.

Introduction

Nanotechnology started to be used fifty years ago because it easy to deal with things at the nanometer scale. Recently, nanotechnology has entered many areas of life, such as biomedicine, food, energy, electronics, textile, environment, solar cells, and hydrogen fuel cells [1]. Carbon is one of the most common elements found on the surface of the earth, and it appears in a variety of forms, namely, carbon nanotubes (CNTs), fluorine, and graphene [2]. In state of Multi-Walled Carbon Nanotubes (MWCNTs), that concerned grate consideration due to the remarkable properties such as extremely light weight, high chemical and thermal stability, and high tensile strength, resistance to basic and acidic media. The MWCNTs also play an important role in preparing nanocomposites and treating water pollution [3-6]. The MWCNTs are produced from various methods including arc chemical vapor deposition (CVD) [6], hydrothermal processes [7], discharge [8], laser ablation [9], etc. To improve the performance of MWCNTs, the decorating them with metal oxides has been widely used due to good merits such as thermal stability and, high mechanical strength. Moreover, the dopants of MWCNTs reduces the band gap, to produce an

effective metal oxide nanoparticle in the ultraviolet and visible region [10]. Among the many metal oxides, nickel oxide (NiO) nanoparticle was used as dopant with MWCNTs to produce a more effective compound. The multi walled carbon nanotubes MWCNTs act as a dispersing agent that prevents NiO nanoparticles from accumulation, which result in increasing the surface area compared to pure NiO. NiO is a transition metal oxide has a cubic structure. It is also a p-type semiconductor material with stable band gap in range of 3.6-4.0 Ev. Although most NiO is used as an antiferromagnetic insulator [11]. The nanoparticle oxides have a high surface area, so they use good carriers, absorbents and catalysts [12]. Recently, the cancer cell is one of the most difficult diseases that the world has faced in recent years due to the increase in the number of cases up to 25 million annually in a year 2015. There are many common methods of treating cancer, such as radiotherapy, surgery, and chemotherapy [13]. MWCNTs work to make cancer drugs accumulate at the tumor site by enhanced penetration effect. Since CNT has high elasticity, good stability, and biocompatibility, it can easily penetrate biological barriers and destroy the contents of the cancer cells [14, 15].

This article includes the synthesis of nanocomposites of Mg-doped NiO and Mg-doped NiO\MWCNT using Sol-Gel method. The structural, optical and morphological properties have been identified via characterization process represented by XRD, FTIR, EDX, FESEM and UV-Vis spectroscopy. The biological activity of the prepared nanostructures was determined by the studying cytotoxicity effect of Mg-doped NiO and Mg-doped\MWCNT nanocomposite against breast cancer (MCF-7) and normal human cells (WRL68) utilizing MTT assay. Besides, the ability of Mg-doped NiO and Mg-doped\MWCNT nanocomposites toward the removing Pb^{+2} ions from aqueous solutions have been assessed. Since, the nanocomposites reveal capability of ROS generation of the Mg-doped\MWCNT.

Experimental Section

2.1. Materials

Magnesium nitrate hexahydrate (Mg $(NO_3)_2.6H_2O$), nickel nitrate hexahydrate ($Ni(NO_3)_2.6H_2O$), ($Mg:NiO_2$ = 6% in mole ratio) and oleic acid ($C_{18}H_{34}O_2$) were bought from Sigma-Aldrich (USA). MWCNTs (purity >95 wt%; diameter ~8-15 nm; length ~10-50 μm; Ash<1.5 wt%) were provided from Cheaptubes.com Grafton (USA). Each solution was prepared utilizing deionized water.

2.2. Treatment of MWCNTs

Treated MWCNTs was achieved by adding o.5 g of Raw-MWCNTs in a mixture of sulfuric acid (95% H_2SO_4) and nitric acid (65% HNO_3) 3:1 in flask of 500 ml. The flask was placed in ultrasonic bath for 30min at temperature 30 ^oC to improve dispersion bandy functionalized MWCNTs (F-MWCNTs). Afterwards, the mixture was then diluted with 400 ml of distilled water and washed several times by using vacuum filtered through micro membrane (0.22μm) made from cellulose nitrate to remove any impurities

from F-MWCNTs. Finally, the filtered products were dried for overnight at 100^{o}C to form treated MWCNTs powder.

2.3. Synthesis of Mg-doped NiO nanoparticles

In this step, the 6% Mg-doped NiO nanoparticle was synthesized by sol-gel process. In this proses, Magnesium nitrate hexahydrate Mg $(NO_3)_2.6H_2O$ and Ethyl alcohol $C_{18}H_{34}O_2$ were added as precursor. Adding 10 g of Mg $(NO_3)_2.6H_2O$ to 50 ml of ethyl alcohol and stirred for 1 h until the mixture dissolve completely. Also, 5 g of Ni $(NO_3)_{2.}6H_2O$ was dissolve in 50 ml of ethylalcohol. The prepared mixture was mixed and stirred together on magnetic stirring for 1 h at temperature 60^{o}C. Afterwards, the Oleic acid was added to the resulting solution slowly with constant stirred to result thick gel. The obtained products of 6% Mg-doped NiO NPs was dried at 100^{o}C for 24h and calcined for 4 h at 600^{o}C.

2.4. Synthesis of Mg-doped NiO/MWCNTs nanocomposite

In order to synthesize 6% Mg-doped NiO\MWCNTs nanocomposite by using 1:1 weight ratio of Mg-doped NiO and MWCNTs. Since, 0.3 g of 6% Mg-doped NiO was dissolved in 50 ml of deionized water with 0.3 g of treated MWCNTs. The mixture was sonication for 15 min and stirred for 30 min at 80 ^{o}C. Added 2 ml of NaOH to the mixture and stirred for another 2h. After that, the resulted mixture was washed and filtered with absolute ethanol and deionized water tow times. The product was dried at 120^{o}C for 3h and calcinated for 2 h at 450^{o}C in an oven.

2.5. Characterization

The crystal structure and crystallite size of the prepared Mg-doped NiO and Mg-doped NiO\MWCNT nanocomposite were identified by X-ray spectrum (XRD-6000, Shimadzu) with Cu Kα radiation source (wavelength of 1.54056 ˚A) at diffraction angle (2θ) from 20° to 80°. The chemical composition and functional groups was determined through the FT-IR technique (8400S, Shimadzu) in the range 4000-400 cm^{-1}. Also, the morphological of the prepared samples was identified by field emission scanning electron microscopy (FESEM) (Hitachi Type S-4160) and quickening voltage (20-30 kV). The UV-Vis absorption spectra of Mg-doped NiO and Mg-doped NiO\MWCNTs hybrid were determined on UV.Vis spectroscopy (1800, Shimadzu, Kyoto, Japan).

2.6. Removal of lead (Pb^{+2}) by using doped NiO and nanocomposite

In this test, stock solution of 1000ppm Pb^{+2} was prepared by dissolving a suitable amount of $Pb(NO_3)_2$ in deionized water. The obtained concentrations were resulted from dilution stock solution of Pb^{+2}. In batch adsorption test, 800 mg of Mg-doped NiO and Mg-doped NiO\MWCNT nanocomposites were added to 50 ml of 20 ppm solution of Pb^{+2}, separately, with stirring at room temperature. After adsorption, the nanocomposite was taken from the solution and the residual Pb^{+2} concentrations were

measured by flame atomic adsorption spectroscopy. Samples withdraw at 0, 3, 6, 9 and 24 h to measure the amount of adsorption and removing percentage (R) of Pb^{+2} by the equation in following [16]:

$R\% = C_o\text{-}C_e/C_o \times 100$ ……. (1)

here, C_o and C_e are the initial and equilibrium concentrations of Pb^{+2} (mg L^{-1}).

2.7. MTT Assay of Determination of antitumor activity

The MTT assay has been used to assess the cytotoxic effect of Mg-doped NiO and nanocomposite materials on different concentrations of *L.camara* crude extracts. The preparation MTT solution was achieved using following procedure: A) Kit content contain 1 ml in 10 vials and solubilization solution 50 ml in 2 bottles. Then B) Protocol of Tumor cells ($1x10^4$ – $1x10^6$ cells\ml) were grown in 96 flat well micro-titer plates, in a final volume of 200 ml culture medium per each well. The using microplate is covered with sterilizing parafilm and shacked gently. The plates were incubated at 37°C for 24h and 5%CO_2. Afterwards, the medium was removed and two-fold serial dilutions of suitable nanostructures (12.5, 25, and 50,100,200,400) µg\ml were addition to the wells. Triplicates were used per each concentration and controls (the cells treatment with serum medium). Then, the plates were incubation at 37°C, 5% CO2 at exposure time 24h. 10µl of prepared MTT solution was addition to each well. Moreover, the plates were incubation at 37°C, 5%CO_2 for 4h. Then, removing the media gradually and 100 µl of solubility solution were added per each well doe 5 min. the absorbance of samples was measured by using the ELISA reader at wavelength 575nm. The resulted data of optical density was submitted to statistical analysis in order to calculate the concentration of required nanostructure to result 50% limitation in cell viability for each cell line.

Results and Discussion

3.1. Structural Measurements

Figure (1) represents the XRD patterns of Mg-doped NiO and Mg-doped NiO\MWCNT nanocomposite. The XRD pattern of Mg-doped NiO displayed diffraction peaks at 2θ = 37.33°, 43.27°, 62.43°, 75.47°, and 79.42° are corresponding to the hkl planes of (202), (111), (220), (311), and (222), respectively. This confirms the formation of cubic structure of NiO. Whereas, the diffraction peaks at 2θ =26.37°, 58.38°, are corresponding to the hkl planes of (111), and (311), respectively which are related to the substitution of the Mg ions for the nickel ions in the NiO compound .[17] The XRD pattern of nanocomposite are displayed two different groups appears in patterns. The peaks at 2θ = 37.41°, 43.46°, 63.02°, 75.52°, and 79.25° are attributed to the hkl planes of (200), (111), (220), (311), and (222) and matches well with nickel oxide structure. These patterns indicate the cubic structure of NiO (JCPDS Card No: 78-0643) [18]. It can be seen that the sample is high crystallized and cubic phase is the only component of the hybrid material. Also, XRD pattern shows diffraction peak at 2θ = 58.54° for (311) with less intensity, corresponding to magnesium ions. This small peak reveals the impregnation of Mg ions on the cubic

surface of NiO structure. Besides, the XRD pattern of nanocomposite reveals a diffraction peak at 2θ = 26.6° of (002) crystal plane related to the graphitic structure of MWCNTs [4, 18]. The average crystal size calculated from Debye-Scherer's equation of Mg-doped NiO and Mg-doped NiO\MWCNT nanocomposites are about 53.33 and 25.43 nm, respectively.

The results of FTIR spectra of Mg-doped NiO and Mg-NiO\MWCNT nanocomposites in a range of 400-4000 cm^{-1} were revealed in Figure (2). FTIR spectrum of prepared Mg-doped NiO sample reveals the appearance of a wide peaks in the range 3435-3437 cm^{-1} due to the stretching vibration of hydroxyl groups. The absorption peaks about 2078-2109 cm^{-1} are due to the stretching vibration of C-H bond of CH_2 and CH_3 groups represented in the FTIR spectra. Conversely, the absorption peaks at 1633-1638 cm^{-1} are due to the bending vibration of the water molecules (H-O-H). The absorption peaks at 1049-1056 cm^{-1} are related to the symmetric stretching vibration of CO_2 groups that adsorbed on the surface of the samples. Finally, the weak absorption peaks around 709-711 cm^{-1} are related to the stretching vibration of the Ni-O bond in doped NiO. The band at 419 cm^{-1} is corresponding to the stretching vibrational mode of Mg-O bond [19-22]. After decorating F-MWCNT with Mg-NiO, it was observed the appearance and disappearance of some absorption peaks in FTIR spectrum. The absorption peaks located at 2925.01cm^{-1} and 2854.96 cm^{-1} are due to the C-H symmetric and asymmetric stretching vibration, respectively due to residual amorphous carbon species. The absorption peak at 2724.11 cm^{-1} is due to the absorption of CO_2 groups. Moreover, absorption peaks appear at 1458.99, 1376.94 cm^{-1} related to C-H and O-H bending vibration, respectively. Finally, weak absorption peaks at 722.08 cm^{-1}, 504.16 cm^{-1} confirm the metal-oxide formation between (Ni-O and Mg-O) [21, 23, 24].

3.2. Morphological Measurements

Figure (3a,b) represents the FE-SEM images of pure NiO NPs and NiO doped with Mg element, respectively. It is observed that pure NiO NPs displays a smooth surface covered with particles of spherical shapes and asymmetric sizes distributed over the surface [25]. FESEM images of the nanocomposite Mg-doped NiO/MWCNTs are shown in Figure (3c,d) with different magnifications. It can be seen that the Mg-doped NiO nanoparticles specially made and attached to the surfaces of treated MWCNTs rather than to other regions without MWCNTs. The FESEM analysis demonstrates the light spots which relate to doped NiO nanoparticles decorated the tubes. As display in these figures, the side walls of MWCNTs are evenly decorated with doped NiO nanoparticles and there are NPs aggregates on the wall of MWCNTs which are so dense and not uniform, that it is hardly to see the hollow cavity of the tubes, which may result from the application of heat for a long time [28]. The particle size mean of Mg-NiO and Mg-doped NiO\MWCNT nanocomposite are about 78.26 nm and 35.02 nm. This confirms the Mg doped NiO nanoparticles and its heterogeneous dispersed on the surface of the F-MWCNTs. The results obtained from the FESEM analysis are similar to a study prepared by **Saravanakkumar et al.** [26], **Karnaukhov et al.** [27], and **Mustafa et al.** [28].

Besides, the EDS spectrum of Mg-doped NiO displays the appearance of oxygen, nickel and magnesium elements, and this indicates that Mg is successfully doped in NiO sites during the chemical reaction formation Mg-NiO. We observe a clear increase in the weight ratio of Mg from 2.78% to 3.48% at high concentration of Mg (except at 4% Mg). In contrast, EDS analysis for Mg-doped NiO\MWCNT nanocomposite is demonstrate in Figure (4 a,b). The EDS analysis confirms the appearance of nickel and magnesium components in the hybrid sample beside to carbon and oxygen. These results indicate the success of forming the Mg-doped NiO\MWCNT nanocomposite. Moreover, the appearance of weak peaks in the EDS spectrum were due to the presence of small content of contaminants such as aluminum (Al, 3.01%), calcium (Ca, 1.21%), and zinc (Zn, 5.26 %)[26].

3.3. Optical Measurements

The optical properties of the prepared colloidal solutions can be identified via UV-Vis spectroscopy in the wavelength range of 200-800 nm, as shwon in Figure (5). The absorption spectrum of Mg-doped NiO shows a broad absorption peak at wavelength of 265 nm. In contrast, the UV-Vis spectra of the Mg-doped NiO\MWCNTs nanocomposite display a shift towards the higher wavelength (red shift) at absorption peak at 361 nm with an apparent higher band intensity [29, 30]. In state of measurement the optical band gap energy (E_g) for all samples can be calculated by Tauc's equation [31]:

$$(\alpha h\upsilon)^2 = A\,(h\upsilon - E_g) \qquad \ldots\ldots\ldots (2)$$

Where hv is the photon energy, E_g is the optical band gap energy, and A is a constant. Figure (6) displays the energy band gap spectrum of Mg-doped NiO and Mg- doped NiO\MWCNTs nanocomposite. Where the energy band gap is estimated by plotting $(\alpha h\upsilon)^2$ against the photon energy ($h\upsilon$) and a linear extrapolating at the absorption edge toward the x-axis. It is observed that the energy gap value (E_g) of the Mg-doped NiO up to 3.28 eV. In contrast, the band gap energy value of the nanocomposite up to 2.82 eV. An obvious decrease in the E_g was observed, which related to the capability of the treated MWCNTs to become as photogenertaed of electron assepters and SPR [32].

3.4. Biological Treatments

Removal of lead nitrate (200 ppm) had been determined by atomic absorption spectroscopy, after incubation at room temperature with 16 g/L of Mg-doped NiO and Mg doped NiO\MWCNTs nanocomposites within 24 h. The percentage of lead nitrate was removed by using the synthesized nanoparticles as shown in Figure (7). The highest percentage of lead removal from watery phase were 62 and 43 performed in the presence of Mg-doped NiO NPs and Mg doped NiO\MWCNTs nanocomposite, respectively, with significant analyses of $P \leq 0.001$ observed in all treatments.

Industrial wastewater commonly includes lead heavy toxic metal that not easily degrade and threat the environment even when presence at low concentration. There are many chemical and physical treatment methods to removal heavy metals from wastes. Adsorption by natural and nanomaterials is one of the attractive approaches to remediate heavy metals. Adsorption efficiency of lead by

nanoparticles depends on the concentration of lead and adsorbent, incubation time, adsorption kinetic and affinity between pollutant and nanomaterial. A significant removal percentage of 65 was observed at pH of 6.0 when the effect dose of nanocomposite was 4 g/L and lead concentration was 100 ppm [33]. On the other studies, equilibrium between lead and NiO was performed (45 % removal) within two hours when lead concentration used at 50 mg /L and NiO, prepared by either organic solvent or precipitate methods, at 25 g/L [15], while 99 % of Pb removal can be performed by 15 g/L of Cr doped NiO NPs, and lead adsorbed higher than other examined ions [34]. On the other hand, many nanomaterials had been developed to remove heavy metals, such as; SWCNTs and MWCNTs, clay, chitosan, and natural zeolite from industrial wastewater [35]. MWCNTs have wide applications in wastewater treatment in additions to other applications. The oxidized form of MWCNTs has been proved to adsorb in high efficiency for heavy metals. The oxygenous functional groups on the MWCNTs surface, provide the MWCNTs a large ability to adsorb lead ions, and it can be seen that in the present study [36-38].

Antitumor activity of Mg-doped NiO and Mg-doped NiO/MWCNTs nanocomposites were measured against MCF-7 tumor cell line and WRL68 normal cell line. The MTT assay was used to determine cell viability of (25, 50, 200 and 400) µg/ml from synthesized nanocomposite after incubated at 37 ●C for 24 h in the presence of 5% CO_2. All tested synthesized nanoparticles were revealed high toxicity with 400 µg/ml against two tested cell lines. Generally, the higher concentration of Mg-doped NiO and nanocomposites, result in the greater the effects on the examined cells. Moreover, the cell viability reached to 70.2%-71.9% in the presence of Mg-doped NiO, while it is about 66.7%- 71.9% in the presence of nanocomposites against MCF-7 and WRL-68 cell lines, respectively, as shown in Figure (8). Based on the results, the tumor can be treated either physically by radiation and hyperthermia, or chemically by intracellular entry of nanoparticles to induce reactive oxygen spices (ROS), and most importantly, the apoptotic, programmed cell death, and necrotic, direct cell damage, in tumor cells populations [13]. The results also reveal capability of ROS generation of the Mg-doped NiO and nanocomposite.

As shown in Figure 9, the increasing ROS levels induce significant damage to the DNA of the cells, resulting in the arrest of cell-cycle and subsequently cell death. The high concentration of Mg-doped NiO might have increased the production of oxygen free radicals within the cells which causes cell death. Besides, the cytotoxic effects of doped NiO NPs are generally resulted by the high level of (ROS) and or less Mg ions. The formation of ROS results in more oxidative stress and oxidant damage in cells. The results suggested that cytotoxicity is related to release Mg-doped NiO from the extracellular degradation of nanocomposite. Cells could also phagocytize high content of 6% Mg-doped, and the MWCNTs released from the intracellular degradation of nanocomposite in the acidic environment of lysosome could also induce cytotoxicity, as shown in Figure 10. As observed, the Figure reveals the morphology of WRL68 cell line when treated with Mg-doped NiO and Mg-doped NiO\MWCNTs nanocomposites, respectively.

Conclusions

The Mg-doped NiO and Mg-doped NiO/MWCNTs were successfully prepared by sol-gel method. The UV-Vis spectroscopy showed that all the prepared samples had a high absorbance and an energy band

gap of up to 2.82 eV. It was observed that the Mg-doped NiO/MWCNTs nanocomposite had good physical stability and a high zeta potential value up to -31mV. The XRD and EDX analysis displayed that the formation of the Mg-doped NiO/MWCNTs nanocomposite, which has a cubic phase and a high crystalline nature. The FE-SEM images confirm the success of deposition of the Mg-NiO on the surface of the treated MWCNTs through the appearance of spherical shapes over the cylindrical tubes. The test for removing lead from water contaminated with Mg-doped NiO and Mg-doped NiO/MWCNTs nanocomposite reveal that the removal percentage of pollutant reaches 43 and 60%, respectively. The Mg-doped NiO and Mg-doped NiO/MWCNTs nanocomposites were showed low cytotoxicity against MCF-7 and WRL68 cell lines.

Declarations

Compliance with ethical standards

Conflict of interest: The authors declare that they have no conflict of interest.

References

1. Poole Jr, C.P. and F.J. Owens, Introduction to nanotechnology. 2003: John Wiley & Sons.

2. Trojanowicz, M., Analytical applications of carbon nanotubes: a review. TrAC trends in analytical chemistry, 2006. **25**(5): p. 480-489.

3. Mirabootalebi, S.O. and G.H. Akbari, Methods for synthesis of carbon nanotubes-Review. Int. J. Bio-Inorg. Hybr. Nanomater, 2017. **6**(2): p. 49-57.

4. Ahmed, D. and A. Abed, Controlled surface modification of CNTs using mild acids through powerful sonication technique. Acta Physica Polonica, 2018. **134**: p. 7-9.

5. Ahmed, D.S., A.J. Haider, and M. Mohammad, Comparesion of functionalization of multi-walled carbon nanotubes treated by oil olive and nitric acid and their characterization. Energy Procedia, 2013. **36**: p. 1111-1118.

6. Allaedini, G., S.M. Tasirin, and P. Aminayi, Synthesis of CNTs via chemical vapor deposition of carbon dioxide as a carbon source in the presence of NiMgO. Journal of Alloys and Compounds, 2015. **647**: p. 809-814.

7. Morais, R.G., et al., Hydrothermal Carbon/Carbon Nanotube Composites as Electrocatalysts for the Oxygen Reduction Reaction. Journal of Composites Science, 2020. **4**(1): p. 20.

8. Zhao, T., et al., Hydrogen storage capacity of single-walled carbon nanotube prepared by a modified arc discharge. Fullerenes, Nanotubes and Carbon Nanostructures, 2017. **25**(6): p. 355-358.

9. Kazeimzadeh, F., R. Malekfar, and M. Houshiar. The effect of graphitic target density on carbon nanotube synthesis by pulsed laser ablation method. in AIP Conference Proceedings. 2018. AIP Publishing LLC.

10. Belin, T. and F. Epron, Characterization methods of carbon nanotubes: a review. Materials Science and Engineering: B, 2005. **119**(2): p. 105-118.

11. Khoshhesab, Z.M. and M. Sarfaraz, Preparation and characterization of NiO nanoparticles by chemical precipitation method. Synthesis and Reactivity in Inorganic, Metal-Organic, and Nano-Metal Chemistry, 2010. **40**(9): p. 700-703.

12. Shajudheen, V.M., M. Sivakumar, and S.S. Kumar, Synthesis and characterization of NiO nanoparticles by thermal oxidation of nickel sulfide nanoparticles. Materials Today: Proceedings, 2016. **3**(6): p. 2450-2456.

13. Vinardell, M.P. and M. Mitjans, Antitumor activities of metal oxide nanoparticles. Nanomaterials, 2015. **5**(2): p. 1004-1021.

14. Dineshkumar, B., et al., Single-walled and multi-walled carbon nanotubes based drug delivery system: Cancer therapy: A review. Indian journal of cancer, 2015. **52**(3): p. 262.

15. Mohammad, R., Duha S. Ahmed, Mustafa KA Mohammed & Mohammad. Chem. Pap, 2020. **74**: p. 197-208.

16. Mohammed, M., M. Mohammed, and D. Ahmed. Effect of Raw-SWCNTs, SWCNTs/Ag-TiO2 nanoparticles for control the biological contaminates in water Treatment. in Journal of Physics: Conference Series. 2021. IOP Publishing.

17. Allaedini, G., P. Aminayi, and S.M. Tasirin, Structural properties and optical characterization of flower-like Mg doped NiO. AIP Advances, 2015. **5**(7): p. 077161.

18. Meybodi, S.M., et al., Synthesis of wide band gap nanocrystalline NiO powder via a sonochemical method. Ultrasonics sonochemistry, 2012. **19**(4): p. 841-845.

19. Lingaraju, K., et al., Biosynthesis of Nickel oxide Nanoparticles from Euphorbia heterophylla (L.) and their biological application. Arabian Journal of Chemistry, 2020. **13**(3): p. 4712-4719.

20. Anand, G.T., et al., Structural and optical properties of nickel oxide nanoparticles: Investigation of antimicrobial applications. Surfaces and Interfaces, 2020. **18**: p. 100460.

21. Budiredla, N., et al., Synthesis and optical characterization of Mg1-xNixO nanostructures. International Scholarly Research Notices, 2012. **2012**.

22. Bhatt, A.S., et al., Chitosan/NiO nanocomposites: a potential new dielectric material. Journal of Materials Chemistry, 2011. **21**(35): p. 13490-13497.

23. Saravanakkumar, D., et al., Structural Investigation on Synthesized Ag Doped ZnO-MWCNT and Its Applications. Journal of Nano science, Nano engineering & Applications ISSN: 2231-1777 (Online), 2018. **8**(2): p. 2321-5194.

24. Soomro, R.A., et al., Electrochemical sensing of glucose based on novel hedgehog-like NiO nanostructures. Sensors and Actuators B: Chemical, 2015. **209**: p. 966-974.

25. Kumar, P.V., A.J. Ahamed, and A. Ravikumar, Synthesis of Mg2+ doped NiO nanoparticles and their structural and optical properties by Co-precipitation method. JOURNAL OF ADVANCED APPLIED SCIENTIFIC RESEARCH, 2020. **2**(2): p. 1-9.

26. Saravanakkumar, D., et al., Synthesis of NiO doped ZnO/MWCNT Nanocomposite and its charecterization for photocatalytic & antimicrobial applications. J. Appl. Phys, 2018. **10**: p. 73-83.

27. Karnaukhov, T.M., et al., Sol–gel synthesis and characterization of the binary Ni–Mg–O oxide system. Journal of Sol-Gel Science and Technology, 2019. **92**(1): p. 208-214.

28. Mohammed, M.K., D.S. Ahmed, and M.R. Mohammad, Studying antimicrobial activity of carbon nanotubes decorated with metal-doped ZnO hybrid materials. Materials Research Express, 2019. **6**(5): p. 055404.

29. Cheng, X., et al., Characterization of multiwalled carbon nanotubes dispersing in water and association with biological effects. Journal of Nanomaterials, 2011. **2011**.

30. Cui, H., et al., Effects of various surfactants on the dispersion of MWCNTs–OH in aqueous solution. Nanomaterials, 2017. **7**(9): p. 262.

31. Soylu, M., et al., Effect of calcination and carbon incorporation on NiO nanowires for photodiode performance. Microelectronic Engineering, 2018. **202**: p. 51-59.

32. Ahmad, M., et al., Graphene–Ag/ZnO nanocomposites as high performance photocatalysts under visible light irradiation. Journal of alloys and compounds, 2013. **577**: p. 717-727.

33. Abd El Fatah, M. and M. Ossman, Removal of heavy metal by nickel oxide nano powder. International Journal of Environmental Research, 2014. **8**(3): p. 741-750.

34. Krishna, Y.S., G. Sandhya, and R.R. Babu, Removal of heavy metals Pb (II), Cd (II) and Cu (II) from waste waters using synthesized chromium doped nickel oxide nano particles. Bulletin of the Chemical Society of Ethiopia, 2018. **32**(2): p. 225-238.

35. Yang, J., et al., Nanomaterials for the removal of heavy metals from wastewater. Nanomaterials, 2019. **9**(3): p. 424.

36. Robati, D., Pseudo-second-order kinetic equations for modeling adsorption systems for removal of lead ions using multi-walled carbon nanotube. Journal of nanostructure in Chemistry, 2013. **3**(1): p. 1-6.

37. Farghali, A., et al., Functionalization of acidified multi-walled carbon nanotubes for removal of heavy metals in aqueous solutions. Journal of Nanostructure in Chemistry, 2017. **7**(2): p. 101-111.

38. Baby, R., B. Saifullah, and M.Z. Hussein, Carbon nanomaterials for the treatment of heavy metal-contaminated water and environmental remediation. Nanoscale research letters, 2019. **14**(1): p. 1-17.

Figures

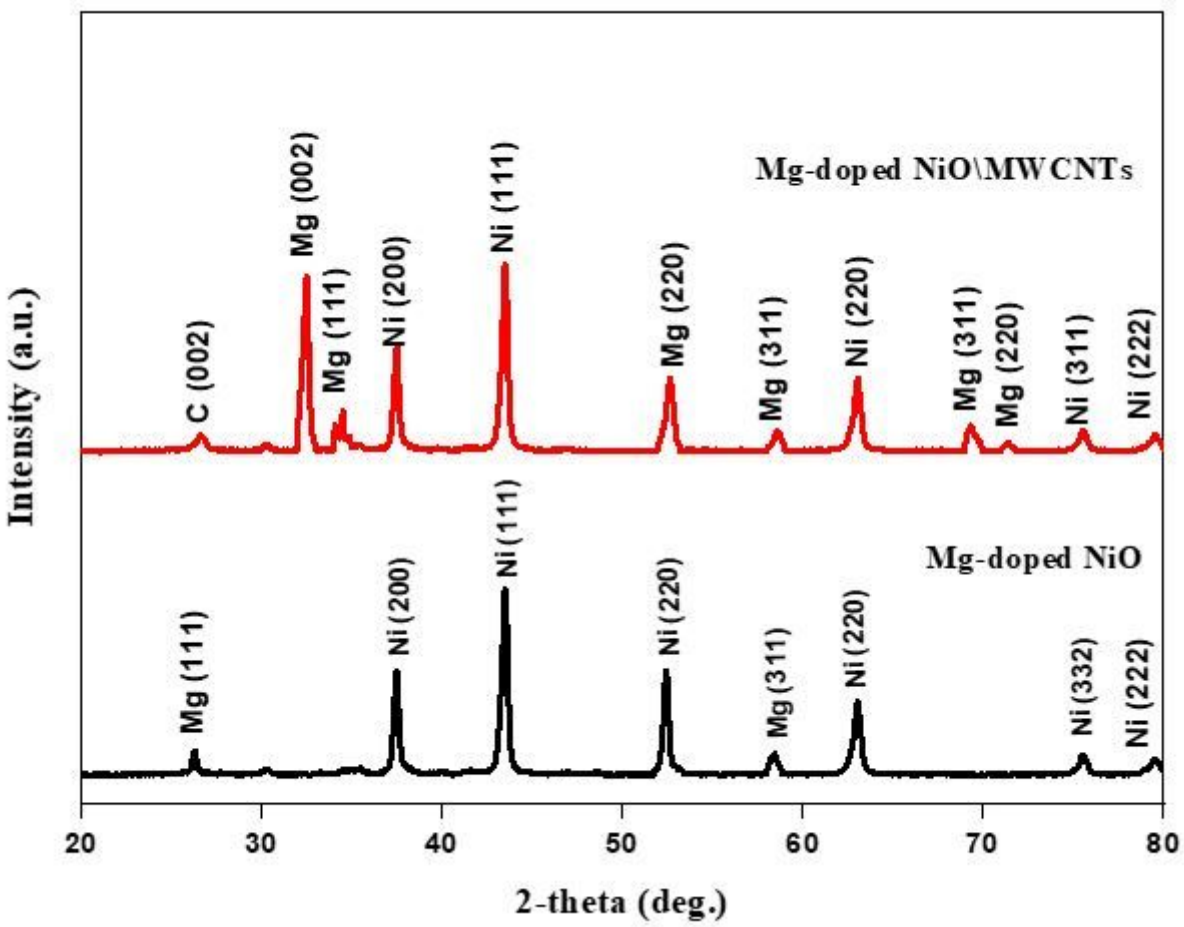

Figure 1

XRD patterns of Mg-doped NiO and Mg-doped NiO\MWCNT nanocomposite

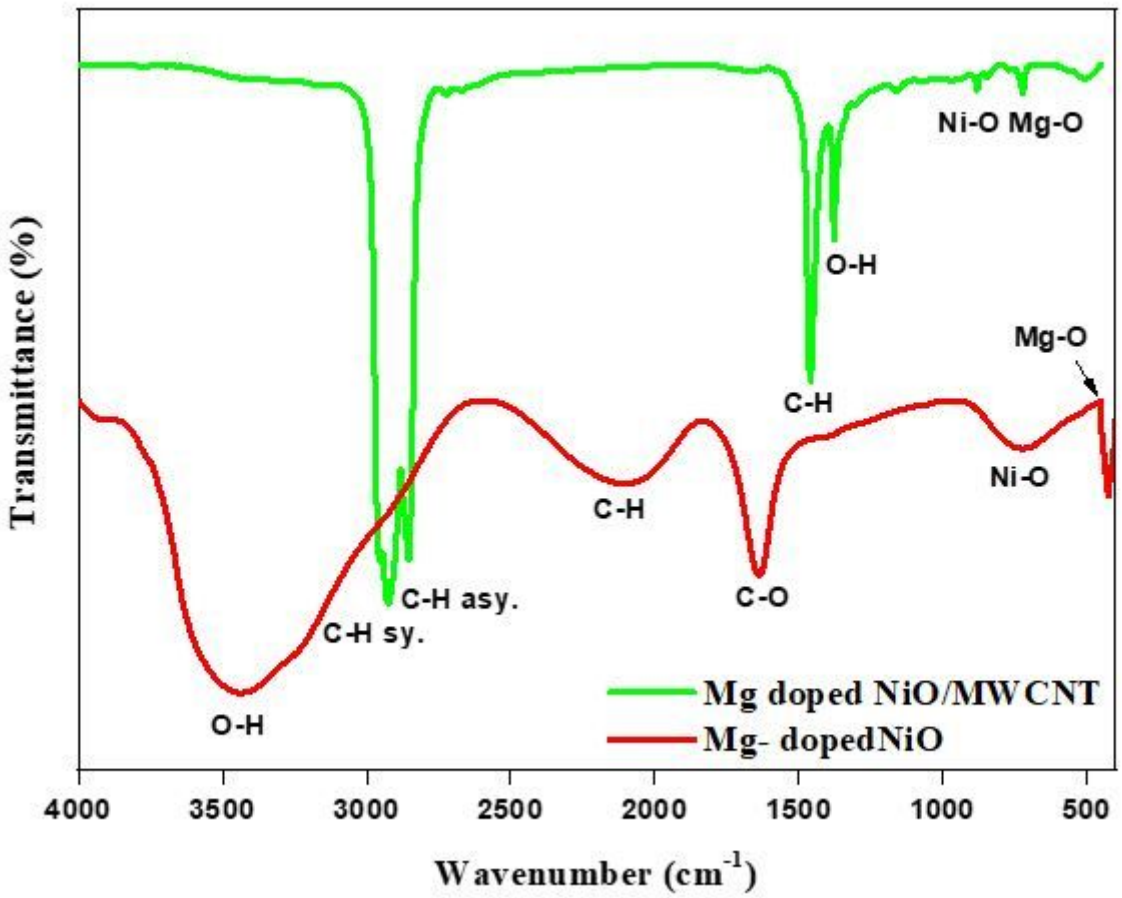

Figure 2

FTIR analysis of Mg-doped NiO and Mg-doped NiO\MWCNT nanocomposite

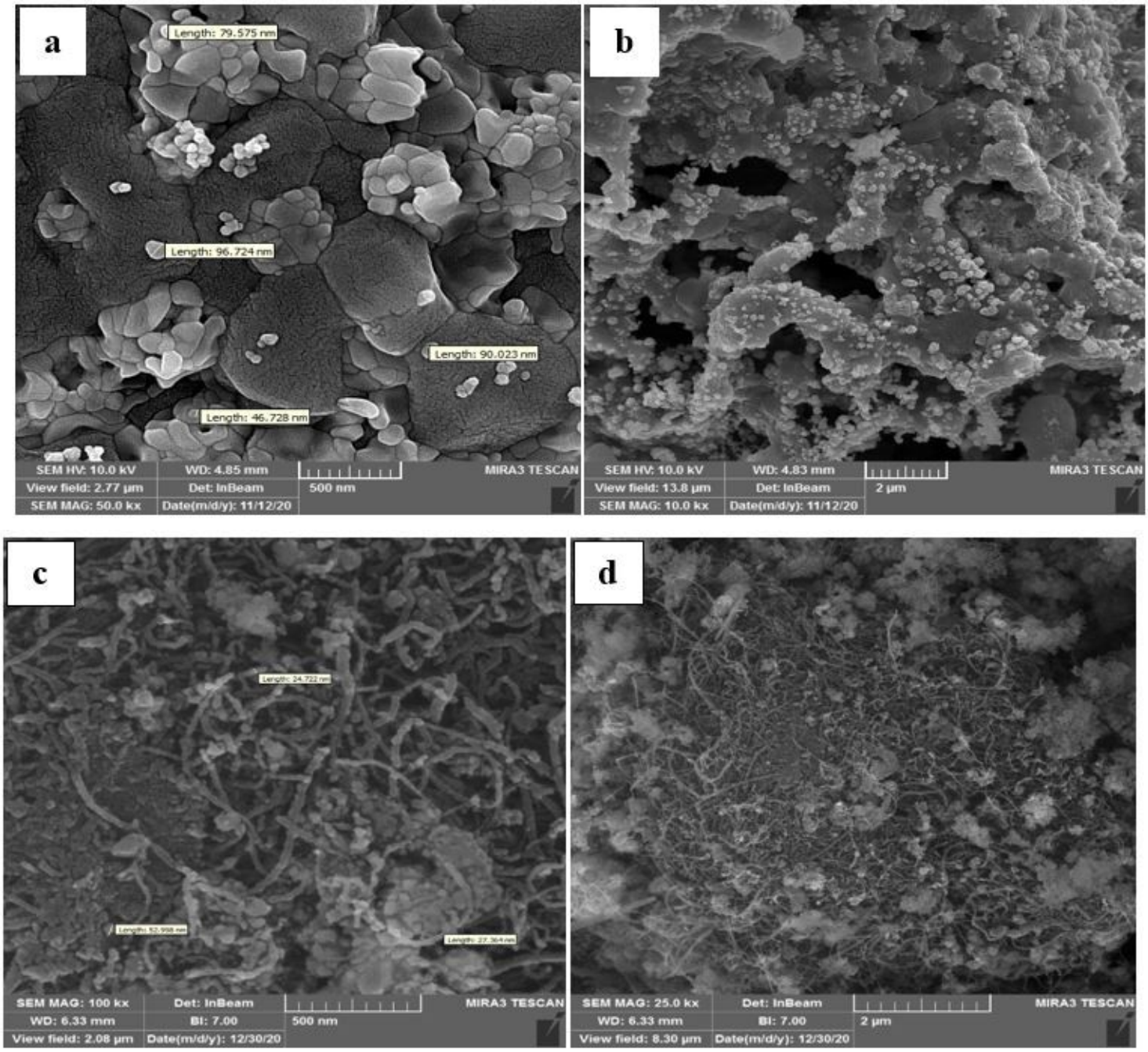

Figure 3

FESEM images of (a, b) Mg-doped NiO and (c, d) Mg-doped NiO/MWCNTs nanocomposite

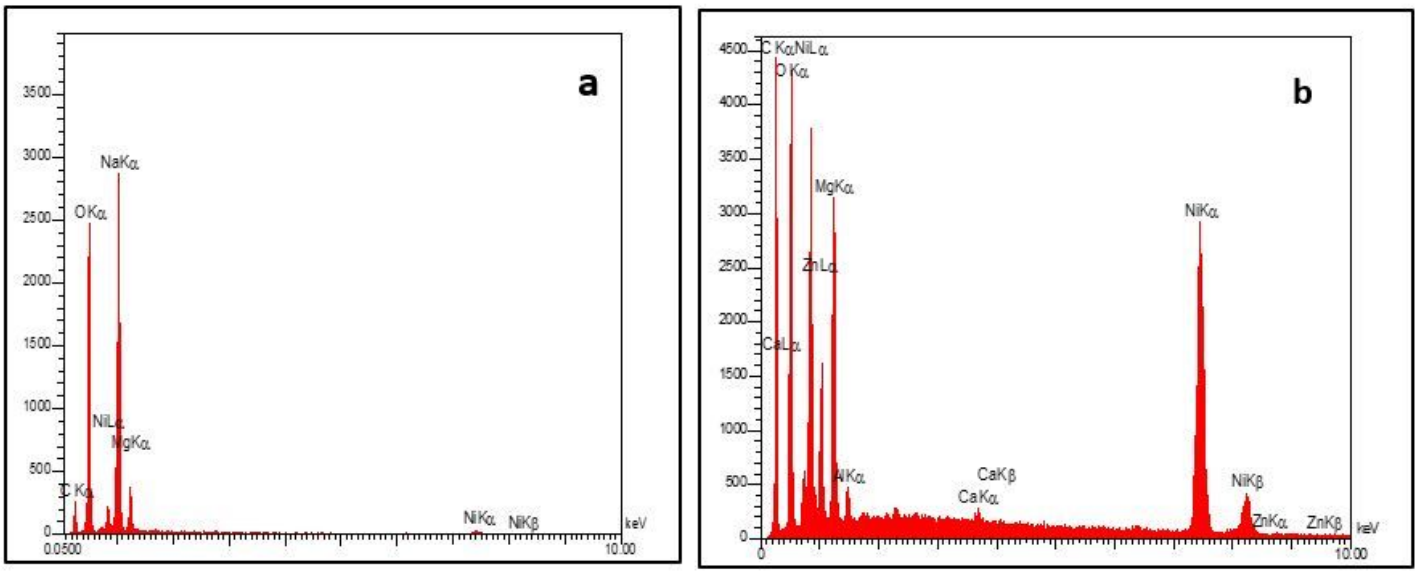

Figure 4

The EDS analysis of a) Mg-doped NiO and b) Mg-doped NiO/MWCNTs nanocomposite

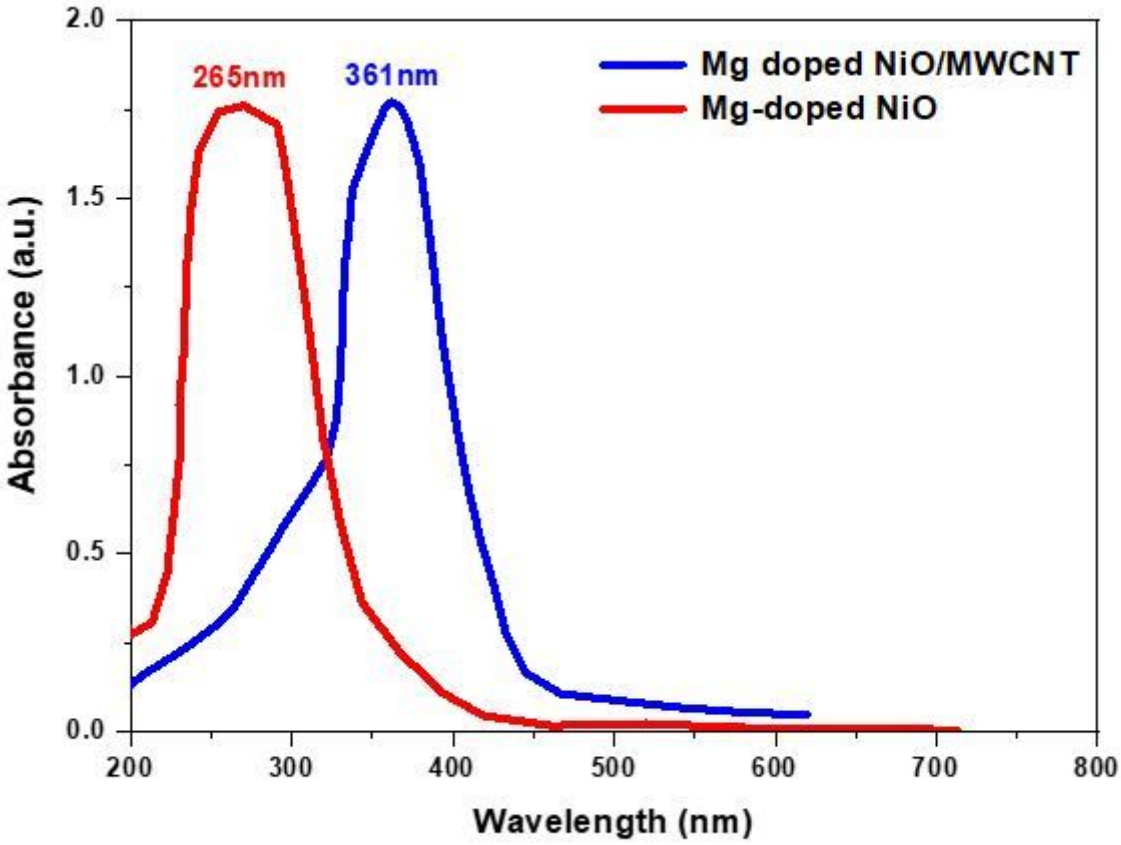

Figure 5

The Optical absorption spectra of Mg-doped NiO and Mg-doped NiO/MWCNTs nanocomposite

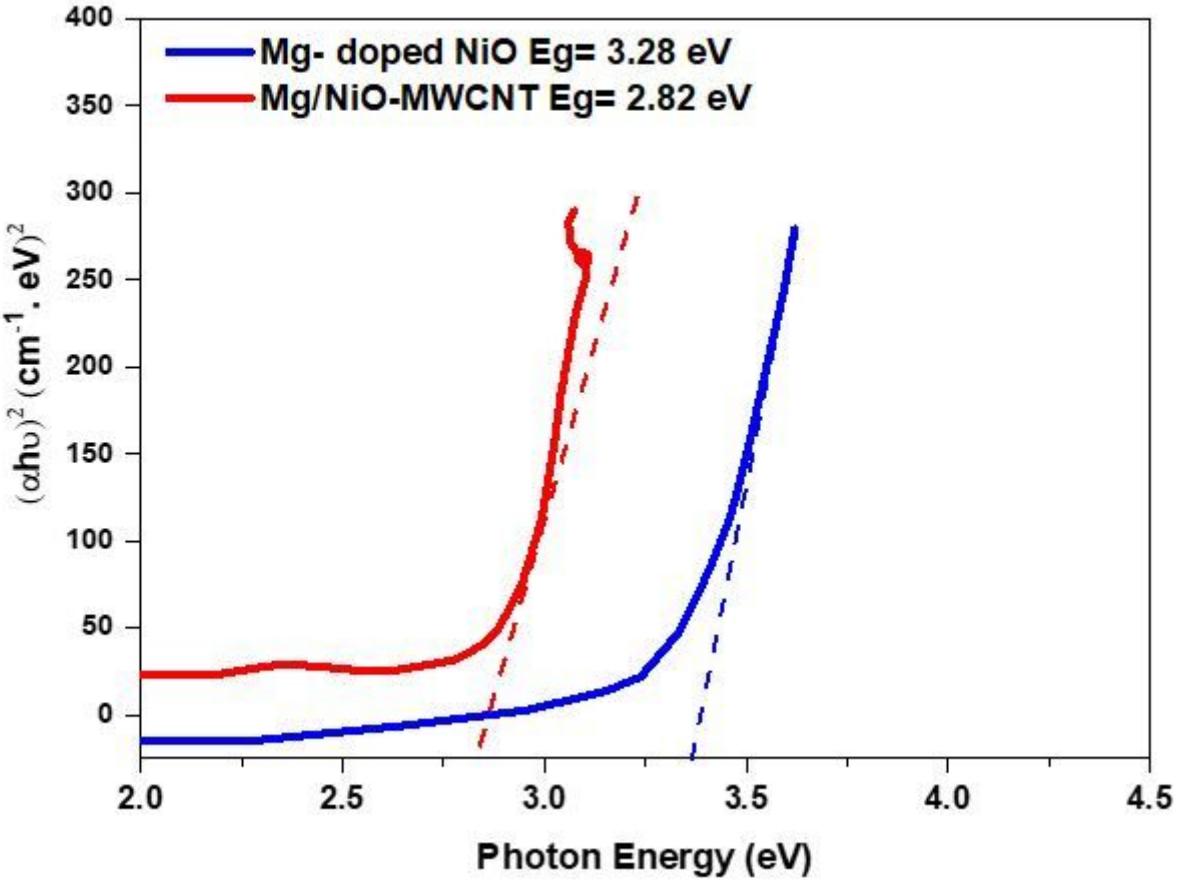

Figure 6

Plot of variation of (αhv)2 vs. photon energy of Mg-doped NiO and Mg-doped NiO/MWCNTs nanocomposite

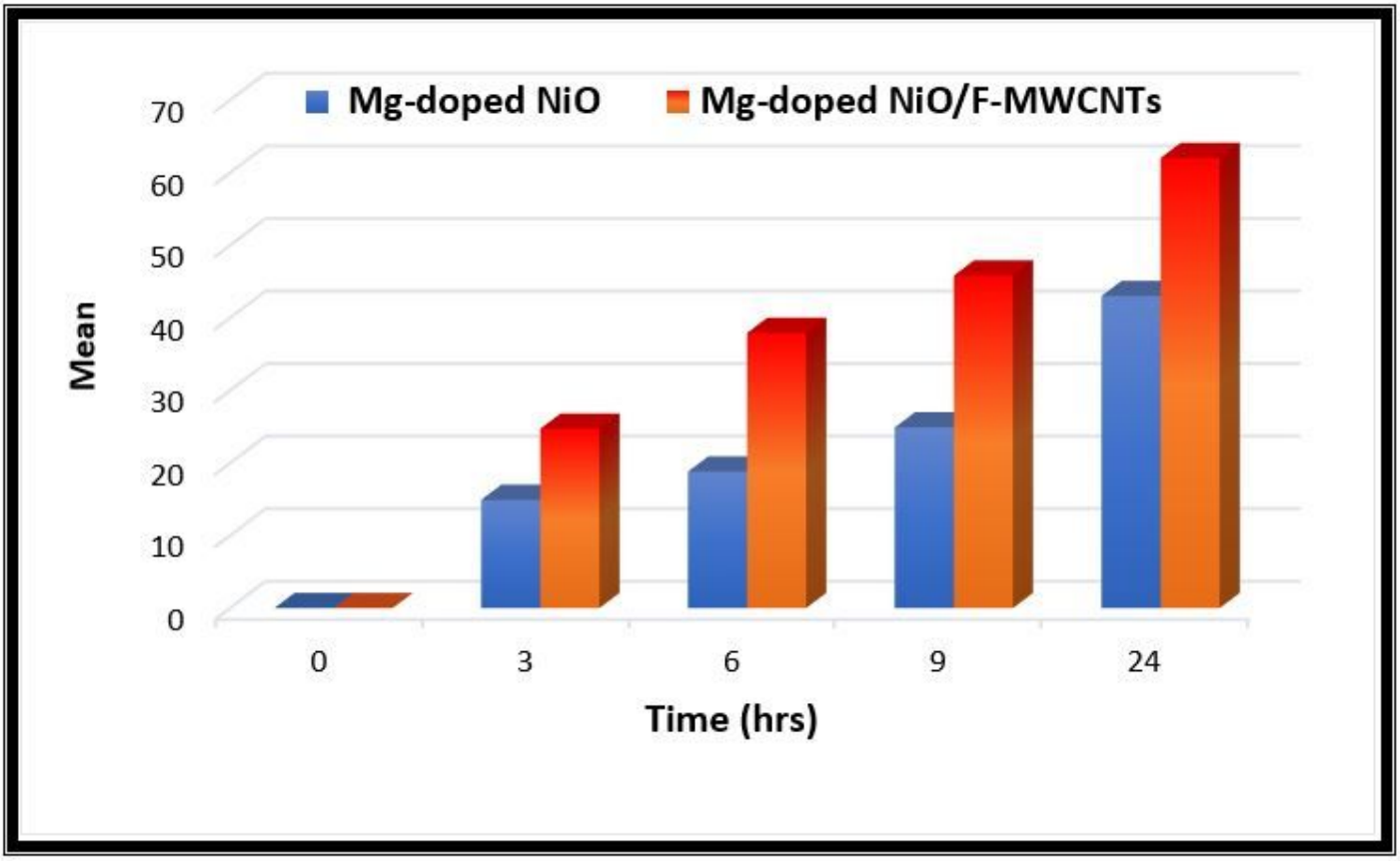

Figure 7

Percentage removal of 200 ppm of Pb(NO3)2 Mg-doped NiO and Mg-doped NiO/MWCNTs nanocomposite within 24 h at room temperature, p≤ 0.001 for all treatments

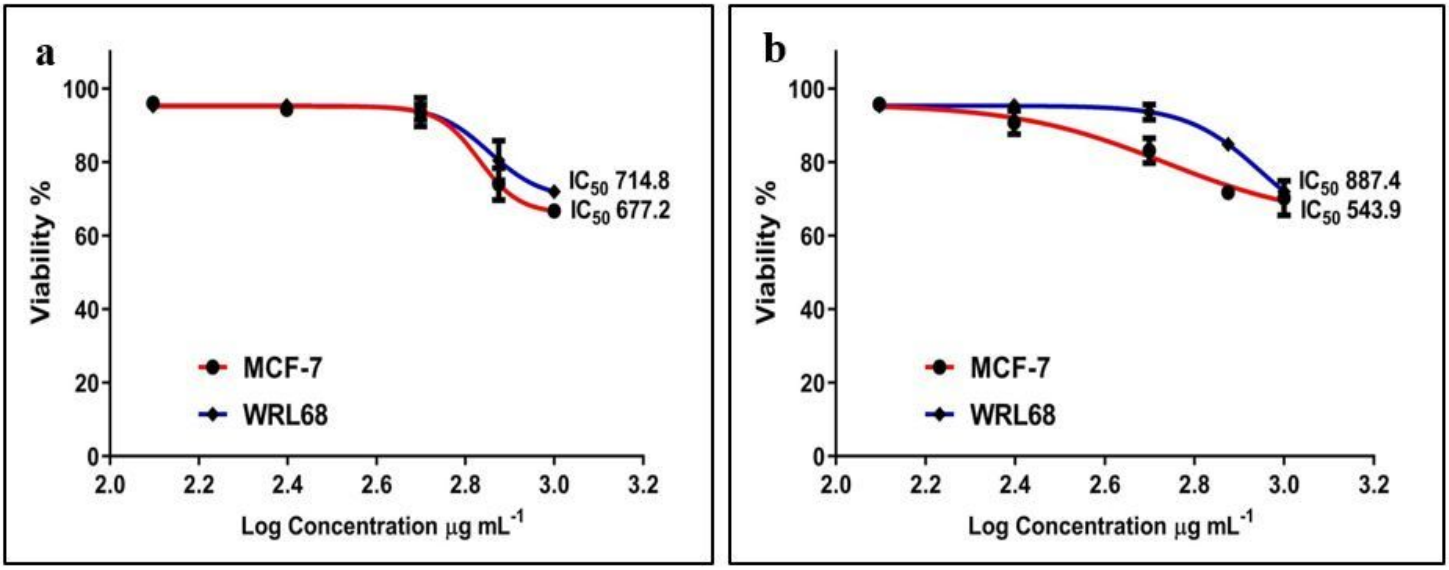

Figure 8

Viability percentage of cell lines in the presence of different concentrations of a) Mg-doped NiO and b) Mg-doped NiO\MWCNTs nanocomposite

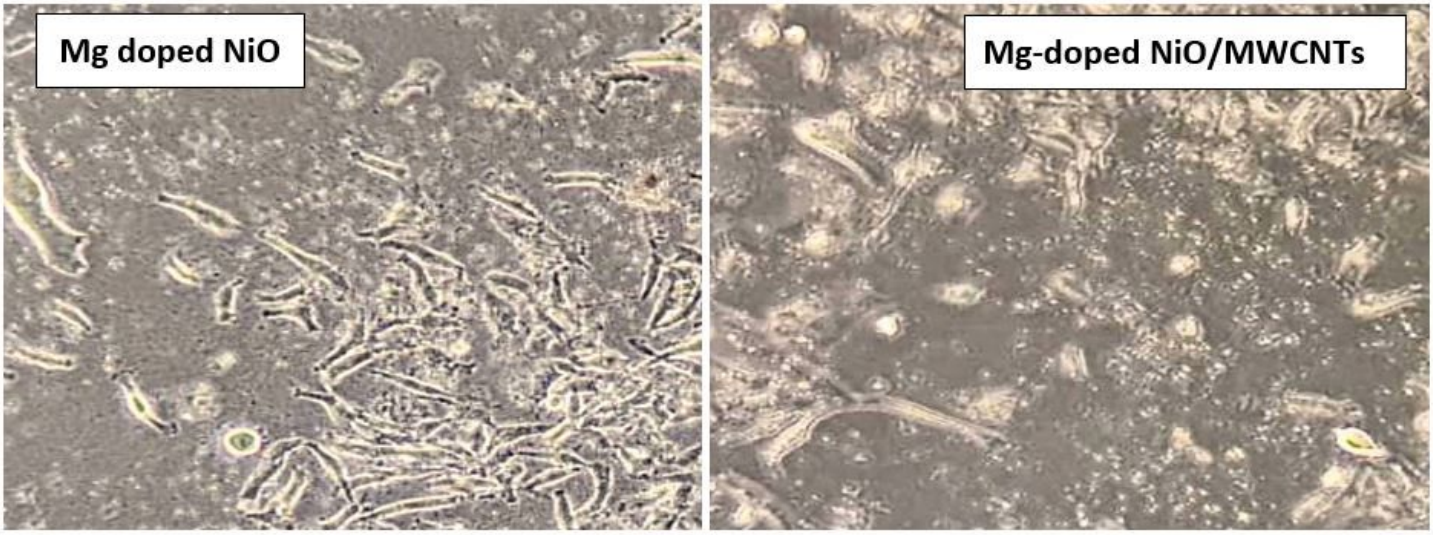

Figure 9

The morphology of viability WRL68 cell line when treated with a) Mg-doped NiO and b) Mg-doped NiO/MWCNTs nanocomposite, after incubated 24hrs

Supplementary Files

This is a list of supplementary files associated with this preprint. Click to download.

- ga.jpg